NRC Research Press

ARTICLE

Climate and bark beetle effects on forest productivity — linking dendroecology with forest landscape modeling

Alec M. Kretchun, E. Louise Loudermilk, Robert M. Scheller, Matthew D. Hurteau, and Soumaya Belmecheri

Abstract: In forested systems throughout the world, climate influences tree growth and aboveground net primary productivity (ANPP). The effects of extreme climate events (i.e., drought) on ANPP can be compounded by biotic factors (e.g., insect outbreaks). Understanding the contribution of each of these influences on growth requires information at multiple spatial scales and is essential for understanding regional forest response to changing climate. The mixed conifer forests of the Lake Tahoe Basin, California and Nevada, provide an opportunity to analyze biotic and abiotic influences on ANPP. Our objective was to evaluate the influence of moisture stress (climatic water deficit, CWD) and bark beetles on basin-wide ANPP from 1987 to 2006, estimated through tree core increments and a landscape simulation model (LANDIS-II). Tree ring data revealed that ANPP increased throughout this period and had a nonlinear relationship to water demand. Simulation model results showed that despite increased complexity, simulations that include moderate moisture sensitivity and bark beetle outbreaks most closely approximated the field-derived ANPP~CWD relationship. Although bark beetle outbreaks and episodic drought-induced mortality events are often correlated, decoupling them within a simulation model offers insight into assessing model performance, as well as examining how each contributes to total declines in productivity.

Key words: ANPP, net ecosystem production, increment cores, forest simulation model, LANDIS-II.

Résumé : Dans les écosystèmes forestiers partout dans le monde, le climat influence la croissance des arbres et la productivité primaire nette aérienne (PPNA). Les effets d'événements climatiques extrêmes (c.-à-d. la sécheresse) sur la PPNA peuvent être aggravés par des facteurs biotiques (p. ex. des épidémies d'insectes). Pour comprendre la contribution de chacune de ces influences sur la croissance requiert de l'information à de multiples échelles spatiales et cela est essentiel pour comprendre la réaction régionale de la forêt au changement climatique. Les forêts mélangées de conifères du bassin du lac Tahoe, en Californie et au Nevada, fournissent une occasion d'analyser l'influence des facteurs biotiques et abiotiques sur la PPNA. Notre objectif consistait à évaluer l'influence du stress hydrique (déficit hydrique climatique, DHC) et des scolytes sur la PPNA à l'échelle d'un bassin de 1987 à 2006. La PPNA a été estimée à l'aide de carotte prélevées sur des arbres et d'un modèle de simulation du paysage (LANDIS-II). Les données dendrométriques révèlent que la PPNA a augmenté durant cette période et qu'elle avait une relation non linéaire avec la demande en eau. Les résultats du modèles indiquent que, malgré l'augmentation de la complexité, les simulations qui incluent un niveau modéré de sensibilité à l'humidité et les épidémies de scolytes produisent la plus proche approximation de la relation entre la PPNA et le DHC dérivée à partir de données terrain. Bien que les épidémies de scolytes et la mortalité épisodique induite par la sécheresse soient souvent corrélées, le fait de les découpler dans un modèle de simulation fournit des renseignements pour évaluer la performance du modèle ainsi que pour examiner de quelle façon chaque facteur contribue au déclin total de la productivité. [Traduit par la Rédaction]

Mots-clés : PPNA, production nette de l'écosystème, carottes de sondage, modèle de simulation forestière, LANDIS-II.

Introduction

Forests are an integral component of the global carbon (C) cycle, sequestering approximately 30% of annual anthropogenic C emissions (Pan et al. 2011*a*). Estimates of forest C dynamics are dependent on reliable forest growth and productivity patterns as influenced by climate and disturbances. Forecasts of forest response to changing future climatic conditions require quantification of the relative importance of key influences on tree growth, mortality, and regeneration, which can vary regionally (Chen et al. 2010; Suarez and Kitzberger 2010; Fisichelli et al. 2012). Regional and local disturbances such as wildfire, drought, or insect outbreaks, which are all influenced by climate variability, will interact to affect future forest dynamics in novel ways. Simulating these interactions is critical for understanding future forest trajectories (Kurz et al. 2008; Adams et al. 2009; Bentz et al. 2010).

Quantifying the response of forest productivity to climate variability and disturbances requires information at multiple scales. Individual tree growth is determined by inter- and intra-annual climate patterns, topographical and edaphic factors, age-related growth patterns, biotic interactions, and disturbances (Fritts and Swetnam 1989). Measures of annual growth increment at the individual tree scale are useful for determining site-specific factors affecting growth. Although abiotic (climatic and edaphic) factors

Received 7 March 2016. Accepted 26 May 2016.

A.M. Kretchun and R.M. Scheller. Portland State University, Department of Environmental Science and Management, P.O. Box 751, Portland, OR, USA.
E.L. Loudermilk. USDA Forest Service, Center for Forest Disturbance Science, Southern Research Station, 320 Green St., Athens, GA, USA.
M.D. Hurteau. University of New Mexico, Department of Biology, Albuquerque, NM, USA.
S. Belmecheri. University of Arizona, Tucson, AZ, USA.
Corresponding author: Alec M. Kretchun (email: aleckretchun@gmail.com).

and endogenous biotic factors (e.g., ungulate browse) may be the primary determinants of growth during early succession (before canopy closure), in more closed canopy conditions, density-related competition may supersede abiotic influences on growth (Hurteau et al. 2007; Kuijper et al. 2010). At the landscape-wide scale, measures of growth help reveal the influence of regional climate patterns such as the Pacific North American pattern, rather than finer scale biotic determinants of productivity such as individual tree competition (Trouet and Taylor 2009).

Individual tree growth is also affected by disturbances in non-uniform ways as a result of physiological responses to stress, damage, or altered stand characteristics. Insects such as bark beetles alter tree growth patterns through increased mortality of older, larger trees, creating canopy gaps and releasing younger cohorts and understory vegetation (Klutsch et al. 2009). Species-specific differences in response to moisture stress can also result in substantial variability in forest growth and carbon (Earles et al. 2014; Hurteau et al. 2007). Moisture stress and bark beetles have also been shown to interact in nonlinear patterns, capable of enhancing or detracting from the effects of the other depending on forest condition and topographic setting (Temperli et al. 2013). The combination of disturbance effects and individual tree species physiological response to changes in climate, particularly severe drought, creates complex overall forest growth patterns.

Although empirically derived relationships (e.g., site index curves) have been used for decades to predict tree growth, modeling forest productivity in a future climate requires capturing the underlying processes that govern regeneration, growth, and mortality (Bontemps and Bouriaud 2014; Gustafson 2013). Models of forest growth must integrate the most influential factors at the scale appropriate for the questions being asked. For instance, site productivity models of even-aged stands may need only basic soils and climate information to approximate observed patterns (Skovsgaard and Vanclay 2008). Ecosystem or landscape models rely on coarse-scale growth responses to temperature and precipitation fluctuations, as well as effects from disturbances (Law et al. 2004; Pan et al. 2011*b*; Scheller et al. 2011; Loudermilk et al. 2013). Coupling fine-scale (individual tree) empirical estimates and landscape-scale model projections of productivity provides an opportunity to compare growth estimations across multiple scales.

The objective of this study was to quantify the influence of moisture availability, as measured by climatic water deficit (CWD), on forest productivity using tree core data and to compare those scaled, in situ estimates of aboveground net primary productivity (ANPP) with outputs from a landscape simulation model (LANDIS-II) to evaluate two factors, moisture sensitivity and bark beetle outbreaks, that influence ANPP in the model. We examined the individual and additive effects from these two factors as simulated by our model and compared simulated ANPP estimates with field-derived estimates of ANPP over a 20 year period. Additionally, we analyzed the merits of each ANPP estimation approach and discuss these in relation to the drivers of forest growth.

Materials and methods

Study area

Our study area consisted of ~31 000 ha of low-elevation forested land within the Lake Tahoe Basin (LTB) on the border of California and Nevada, USA (Fig. 1). The climate is Mediterranean, with dry summers and precipitation, primarily winter snow, occurring mostly from October to May. Temperature and precipitation are largely controlled by the basin-like topography, which ranges in elevation from 1897 m (lake level) to 3320 m; seasonal high and low temperatures decrease with increasing elevation. Soils are primarily of shallow granitic substrate with ancient volcanic bedrock lining

Fig. 1. Study area map. Dots signify field site locations of tree core sampling, the orange area represents LANDIS-II modeling extent, and the grey area is the entire Lake Tahoe Basin.

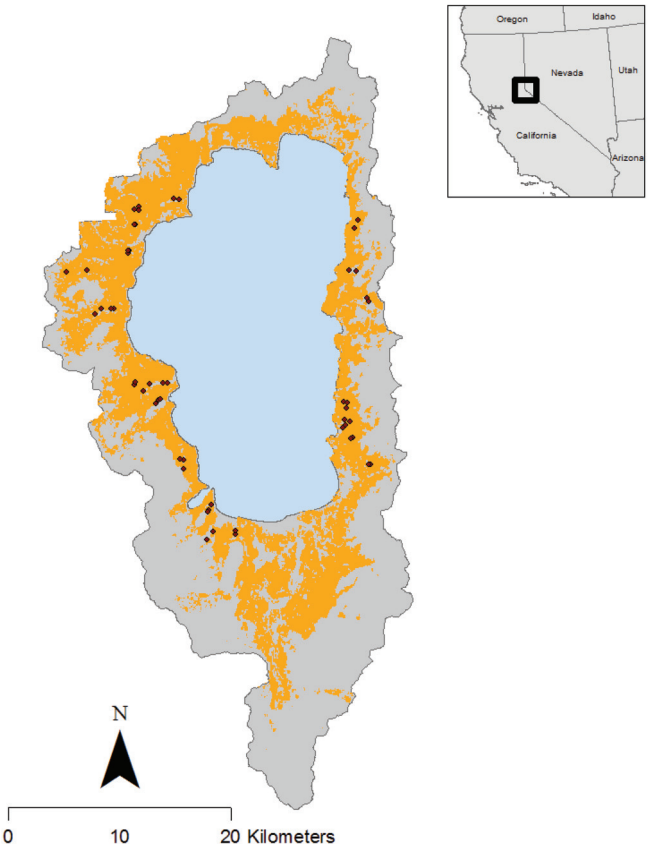

the north shore (Rogers 1974). Primary tree species include Jeffrey pine (*Pinus jeffreyi* Balf.), sugar pine (*Pinus lambertiana* Douglas), white and red firs (*Abies concolor* (Gordon & Glend.) Lindl. ex Hildebr. and *Abies magnifica* A. Murray, respectively) and, to a lesser extent, incense cedar (*Calocedrus decurrens* (Torr.) Florin), whitebark pine (*Pinus albicaulis* Engelm.), western white pine (*Pinus monticola* Douglas ex D. Don), and lodgepole pine (*Pinus contorta* Douglas ex Loudon) (Graf 1999). Within the basin, there are several distinct forest types, including mixed conifer – white fir stands (lake level to ~2100 m elevation), Jeffrey pine dominated stands (lake level to ~2400 m), mixed red fir – western white pine stands (~2100 to ~2600 m), lodgepole pine dominated stands (~2400 to 3320 m), and subalpine stands of whitebark pine or mountain hemlock (*Tsuga mertensiana* (Bong.) Carrière) (~2600 to 3320 m). Old-growth stands and stands dominated by sugar pine exist within the LTB but are rare. Extensive logging during the 19th century, followed by aggressive fire suppression activities, have shifted the forest structure towards dense, young forests (<120 years old) (Beaty and Taylor 2008).

Tree ring estimates of ANPP

We used field data collected at two to four plots in each of 21 creek drainages (52 total plots) ranging from 1900 to 2200 m elevation during summer 2009 to develop our empirical ANPP estimate (Fig. 1) (Supplementary material A, Table S1[1]). Forest structural attributes were measured using a nested design in which all trees ≥80 cm diameter at breast height (DBH, 1.3 m) were measured in a 0.2 ha plot, all trees ≥50 cm DBH were measured in a 0.1 ha subplot, and all trees ≥5 cm DBH were measured in a 0.02 ha subplot,

[1]Supplementary data are available with the article through the journal Web site at http://nrcresearchpress.com/doi/suppl/10.1139/cjfr-2016-0103.

Fig. 2. Temperature, climatic water deficit (CWD), and total precipitation for the Lake Tahoe Basin for the study period of 1986–2007. Temperature and precipitation data were estimated by 4 km Parameter–elevation Relationships on Independent Slopes Model (PRISM) data, averaged across 18 tiles; CWD data are the mean of the Basin Characterization Model tiles. For temperature, dotted lines above and below the mean temperature represent mean annual maximum temperature and mean annual minimum temperature, respectively.

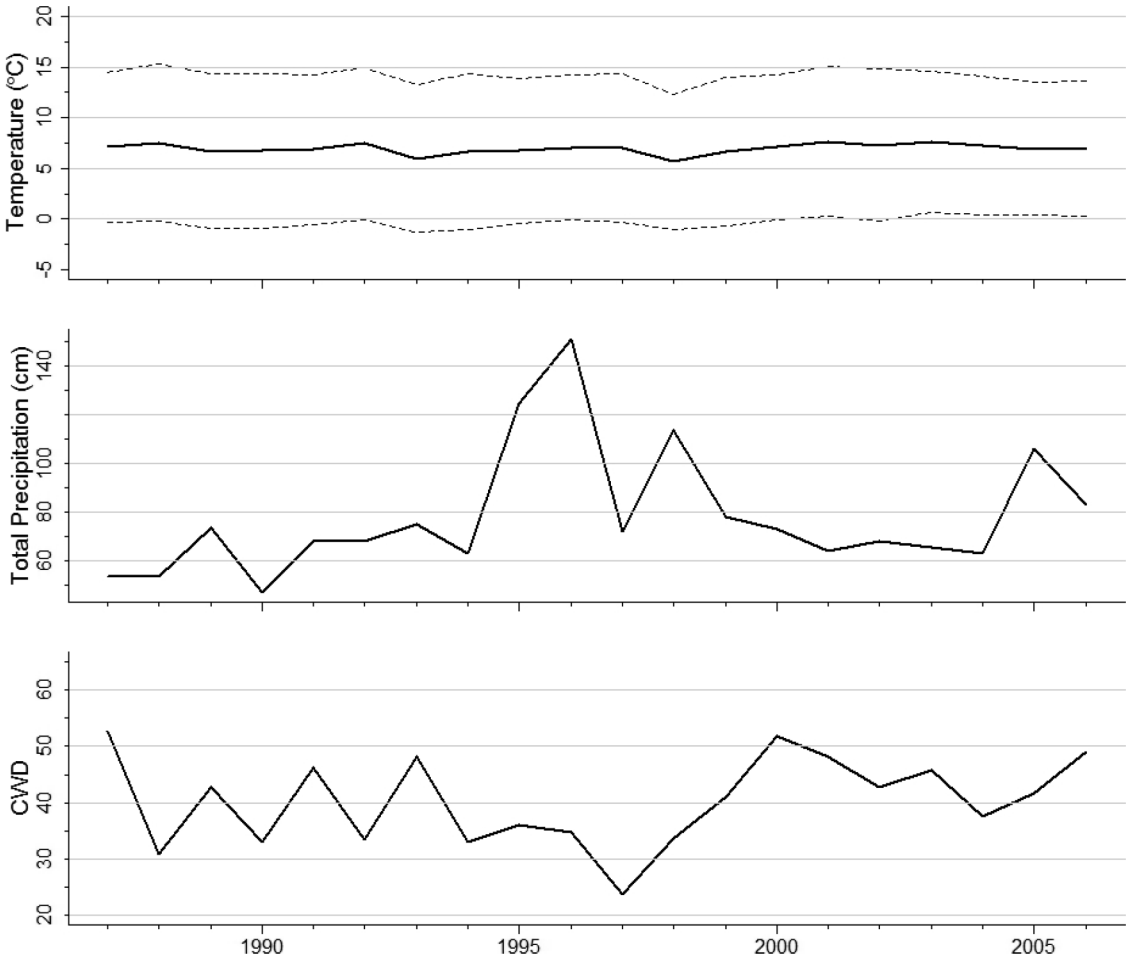

all with the same plot center. Within each plot, two to three individual live trees were selected for coring from the five smallest and five largest individuals (Hurteau et al. 2014). Visual cross dating of tree cores was conducted using characteristic rings and checked with COFECHA (Stokes and Smiley 1968; Holmes 1983). Summary statistics were calculated using the dplR package in R and are presented in Supplemental material A, Table S2[1] (R Core Team 2015; Bunn et al. 2015). The cored tree sample size by species approximated the proportional contribution of each species to mean basal area after excluding cores that could not be cross-dated (Supplementary material A, Table S3[1]).

Annual ring widths were measured to the nearest 0.001 mm using WinDENDRO (Regent Instruments Inc.), and error-prone cores were remeasured using a Unislide TA measuring system (Velmex, Bloomfield, New York). A total of 275 cross-dated raw tree-ring widths were then used to calculate the radius of each tree to account for cores that missed pith. To estimate ANPP for each tree, the inferred radius from the annual increment was then used to estimate DBH for each tree at each annual increment. Annual DBH values were then used to estimate annual biomass production ($kg \cdot ha^{-1} \cdot year^{-1}$) using allometric equations from Jenkins et al. (2004).

To scale tree-level estimates of annual biomass production to the plot level, we matched individuals for which only DBH had been measured with cored individuals of the same species and similar diameter from the nearest plot. Growth patterns for uncored trees were assumed to be similar to cored individuals; annual increment data used from nearby plots had Pearson's correlation coefficients ≥ 0.9 (Supplementary material B, Table S4[1]). Annual growth measurements from the cored individuals and genus-specific allometric equations were then used to estimate annual biomass production for the trees that were not cored. Plot-level estimates of annual ANPP were then scaled to the hectare level using the appropriate scaling factor (e.g., a tree >50 cm DBH represents 50 $trees \cdot ha^{-1}$) from the nested plot design. Empirical ANPP estimates excluded trees <5 cm DBH in 2009 and any dead trees sampled within the plots. Mean basal area by species by sampling area for both live and dead trees is presented in the Supplemental material A, Tables S5 and S6[1].

Climate variables

We selected the period from 1987 to 2006 because it had the highest number of available tree core samples and high resolution data of a large basin-wide bark beetle outbreak that began in 1988 (discussed below). Over the study period, maximum summer temperature ranged from 14 to 18.5 °C, and minimum January temperature ranged from –4.2 to 0.8 °C, according to the 4 km Parameter–elevation Relationships on Independent Slopes Model (PRISM) dataset (Daly et al. 1997). Total annual precipitation ranged from 46.9 cm in 1991 to 151.0 cm in 1997 (Fig. 2).

To estimate moisture demand and evaluate the influence of climate on basin-wide ANPP, we used climatic water deficit (CWD; the difference between actual and potential evapotranspiration),

as estimated by the USGS California Basin Characterization Model (BCM) (Flint and Flint 2012; Flint et al. 2013). BCM combines downscaled 4 km PRISM climate data with physical hydrological process models and produces water balance fractions (e.g., runoff, evapotranspiration, and soil storage) at the HUC-8 basin scale. Each model output variable is produced by BCM at a spatial grid size of 270 m × 270 m, a meaningful scale for site-level analysis. Monthly CWD values for the LTB (#16050101) for the years 1987–2006 were obtained from the USGS California Landscape Conservation Cooperative (2015). Higher CWD values indicate periods of greater moisture deficit. For the period of study, CWD values ranged from a high of 52.7 in 1988 to a low of 23.7 in 1998 (Fig. 2).

Landscape projections of ANPP

We used the landscape disturbance and succession model, LANDIS-II, to model ANPP across the LTB (Fig. 3) (Mladenoff et al. 1996; Scheller et al. 2007). The LANDIS-II model was previously parameterized for the LTB to simulate landscape carbon dynamics under contemporary and future changing climate (Loudermilk et al. 2013, 2014). LANDIS-II is a spatially explicit, raster-based process model and represents trees in species–age cohorts. The model incorporates tree species life history attributes (e.g., longevity, shade tolerance, drought tolerance, seed dispersal distance, etc.) that allow each species to respond uniquely to light, nutrient, and water availability, local climate, soil conditions, and disturbance. LANDIS-II has been applied in many forested ecosystems (Swanson 2009; Cantarello et al. 2011, Gustafson and Sturtevant 2012) and calibrated using a variety of available resources, including eddy flux towers (Scheller et al. 2011) and FIA-derived biomass estimates (Thompson et al. 2011). ANPP calibration in the LTB (Loudermilk et al. 2013) was based on literature values of ponderosa pine plantations in the Sierra Nevada (Campbell et al. 2009).

Century Succession extension

Carbon dynamics were modeled using the Century Succession extension (henceforth referred to as "Century") for LANDIS-II, which is based on the CENTURY soil model (Parton et al. 1983). Century was calibrated and validated with available data to satisfy five model output targets: ANPP, net ecosystem production (NEP), aboveground live biomass, soil organic C (SOC), and soil inorganic nitrogen (mineral N) (Loudermilk et al. 2013). Further details on model development, parameterization, and calibration are in Loudermilk et al. (2013), as well as in the Supplementary materials A and B[1].

Century utilizes monthly climate data, which influences tree establishment, growth, and regeneration (Scheller et al. 2011). The individual species' growth response to available soil moisture is dictated by two parameters; these parameters are assigned to broader functional groups to which each species belongs and dictate moisture sensitivity by determining the ratio of available water content to potential evapotranspiration. The first parameter ("DroughtIntercept" in Century: "pprpts2") determines the effect of available water content on the intercept of this relationship; therefore, if this value is increased, the intercept is raised and a higher available water content is required to achieve the same potential evapotranspiration. The second parameter ("DroughtRatio" in Century: "pprpts3" is the minimum ratio of available water content to potential evapotranspiration at which there is no restriction on production, effectively determining the minimum available water content necessary for any growth to occur. The LANDIS-II Century extension requires calibration of these moisture-related parameters to accommodate unique species and soil combinations.

We simulated two levels of tree moisture sensitivity and two levels of bark beetle occurrence (with and without bark beetles, extension discussed below). We developed two levels of moisture sensitivity (low and high) by leaving the DroughtIntercept parameter constant and iteratively increasing and decreasing the DroughtRatio parameter by the minimum amount (0.1) demonstrated to have a significant effect on the response variable (ANPP), because this parameter is not empirically derived. "Significant effect" in this context is defined as 50% increase or reduction in ANPP, well above the tolerance of the calibration targets in Loudermilk et al. (2013). We simulated two levels of DroughtRatio with both levels of bark beetle occurrence, and the scenarios were named as follows: low moisture sensitivity with no beetles (LowM-noBB), low moisture sensitivity with beetles (LowM-BB), high moisture sensitivity with no beetles (HiM-noBB), and high moisture sensitivity with beetles (HiM-BB).

Fig. 3. Conceptual diagram of LANDIS-II.

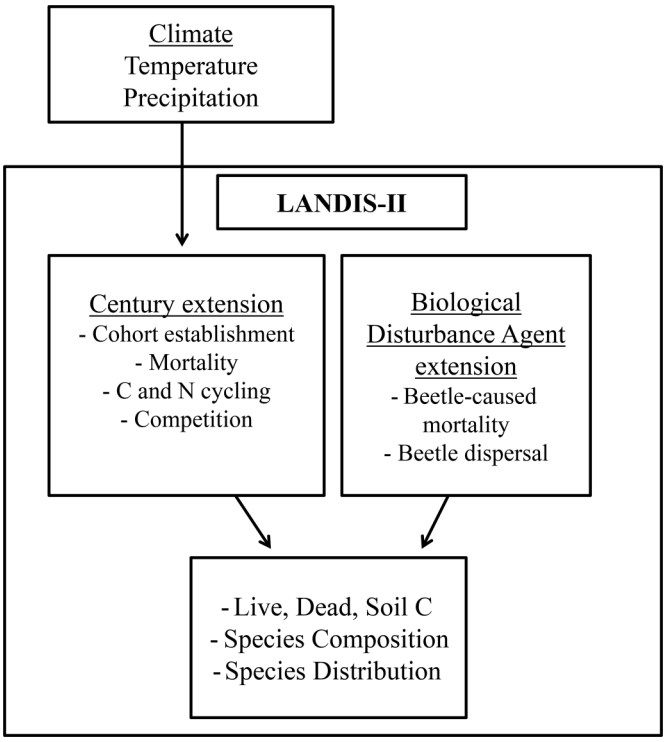

Using LANDIS-II, we ran five replicate 20-year simulations of each scenario for the 31 291 ha study area using a 100 m × 100 m grid and climate data from 1987 to 2006. Monthly temperature and precipitation values for 1987–2006 were from the PRISM dataset for the LTB, at a 4 km resolution (18 PRISM tiles total across the study area). Although forest thinning operations and wildfires occurred in the LTB during the 1987–2006 timeframe, there were no records or physical evidence of any recent fire (wildfire or prescribed burning) or thinning at the field locations where tree cores were collected. We excluded these disturbances from our simulations to be congruent with field site disturbance history over the study period.

Biological disturbance agent (BDA) extension

Bark beetle outbreaks were simulated using the BDA extension for LANDIS-II (Sturtevant et al. 2004). This extension simulates tree mortality that results from outbreaks of insects and disease. We parameterized host species preferences for three bark beetle species active in the LTB and deterministically set the length and initiation year of a simulated outbreak using a documented outbreak in the LTB that began in 1988. BDA does not utilize climate data to influence beetle activity; within this study, it is used as a species-specific stochastic mortality agent parameterized and calibrated to match observed patterns of historical beetle disturbance. The details of this extension and its parameterization are discussed briefly below and in detail in the Supplementary materials A and B[1].

Three bark beetle species were modeled: the Jeffrey pine beetle (*Dendroctonus jeffreyi* Hopkins, 1909; JPB), the mountain pine beetle

(*Dendroctonus ponderosae* Hopkins, 1902; MPB), and the fir engraver beetle (*Scolytus ventralis* LeConte, 1868; FEB). Although there are other beetles active in the area (e.g., red turpentine beetle, *Dendroctonus valens* LeConte, 1860), the three aforementioned beetles are responsible for the majority of the recorded damage in the LTB, and there is very little overlap in host species. Empirical data from the literature and expert opinion were used to determine host species and ages most preferred by each of the three modeled beetle species (Supplementary material A, Table S7[1]). JPB and FEB are limited in their primary host selection (Jeffrey pine and red or white firs, respectively), whereas MPB is more of a generalist, impacting a variety of pine species across the basin (Cole and Amman 1980; Ferrell 1994; Bradley and Tueller 2001; Walker et al. 2007; Egan et al. 2010). Beetle dispersal is modeled within BDA, defined at an annual rate ($m \cdot year^{-1}$).

A widespread outbreak of bark beetles occurred in the region, concurrent with a severe drought that began in 1988. USFS aerial detection survey maps of the basin indicated >15 000 ha of damaged area during the peak year of the outbreak, i.e., 1993. Aerial detection survey maps include attribution of damage to specific beetle species on an annual basis, allowing us to use these survey data to calibrate each of the three beetle species modeled in this study. The total forest area impacted over the study period for each beetle species was 15 785 ha: MPB, 933 ha; JPB, 3126 ha; and FEB, 11 726 ha.

Within BDA, outbreaks are probabilistic at the site level, where the probability of a site being disturbed is based on the available hosts within site, as well as neighboring host resources. Individual host tree species are ranked (primary, secondary, minor, and nonhost) and described by both species and age. For instance, in the LTB, the JPB is an obligate of Jeffrey pine, though it prefers older cohorts (>60 years, primary host) much more than younger cohorts (<20 years old, minor host) (Egan et al. 2010). These host categorizations help determine site vulnerability (Sturtevant et al. 2004). The severity of a simulated outbreak is a function of site vulnerability, which is classified as light, moderate, or severe. A light outbreak kills all vulnerable tree cohorts, a moderate outbreak kills all tolerant and vulnerable tree cohorts, and a severe outbreak kills resistant, tolerant, and vulnerable tree cohorts. Outbreaks are synchronous across a landscape, and severity can be bounded by defining a minimum and maximum possible outbreak severity. The BDA extension reduces site and landscape ANPP through mortality of affected cohorts rather than direct reductions in cohort growth rates.

Tree ring and model estimate comparison

We calculated median ANPP values and 95% confidence intervals from empirical data using bootstrapping with 500 draws from all field sites (tree ring derived ANPP estimates) and by using all grid cells from each scenario (31 291 grid cell landscape) for median values and confidence intervals from the simulation outputs. All replicate outputs for a particular modeling scenario were combined, such that all statistical analyses were applied to a sample consisting of all five replicates simultaneously. Median ANPP values were also used to construct statistical relationships for each ANPP estimation method and the BCM-estimated annual mean CWD. Regressions were constructed using a linearization technique for estimating regression lines with one or more unknown break points (Muggeo 2003). Upper and lower limits of these piecewise regressions were set at the minimum and maximum CWD values (23.6 and 52.7, respectively) for the study period. The number of break points was determined by the number of integers (29) between the minimum and maximum CWD values. ANOVA was used to compare ANPP above and below the CWD breakpoint value identified by the piecewise regression within each model scenario. In the ANOVA test, ANPP was the response, whereas CWD was used as the predictor with an interaction term designating above or below the CWD threshold. Two ANCOVA tests were used to compare the slopes of ANPP~CWD relationships between scenarios. In the ANCOVA tests, the five scenarios were evaluated by statistically comparing the slope of the ANPP~CWD relationship between each scenario above (test 1) and below (test 2) the CWD threshold. All statistical and graphical analyses were done using the R statistical software platform (R Core Team 2015; Bivand et al. 2015; Hijmans 2015; Wickham 2009).

Results

Median ANPP derived from tree cores was generally less than 200 g $C \cdot m^{-2}$ (Fig. 4), with increasing variance over the 20 year study period. Over the study period, median ANPP values increased from 118.5 g $C \cdot m^{-2}$ in 1987 to 207.1 g $C \cdot m^{-2}$ in 2006, with temporal fluctuations throughout the 20 year period. Following a year of particularly high CWD in 2000, median ANPP dropped from 229.4 g $C \cdot m^{-2}$ in 2000 to 150.2 g $C \cdot m^{-2}$ in 2001. The overall increasing trend in ANPP is, in part, a function of an overall growth rate increase following the cessation of basin-wide logging in the 1880s (Loudermilk et al. 2013).

Simulated median ANPP values for all scenarios except LowM-noBB fell within the bootstrapped confidence interval of the tree ring derived data for all 20 years of the study (Fig. 4). The LowM-BB and HiM-noBB median ANPP values were more consistent with empirical values over the study period than the LowM-noBB and HiM-BB scenarios. Consistent with the empirical data, median simulated ANPP values declined sharply in 2001 (Fig. 4), which corresponded with high CWD (Fig. 2; in 2000, CWD = 51.8; in 2001, CWD = 49.0). Confidence intervals for the empirical data were much larger than those of any of the model scenarios, likely because of the discrepancy in sample size between the empirical (n = 52 plots) and modeled (n = ~31 000 grid cells) data.

Median annual ANPP showed a nonlinear relationship with CWD. ANPP had a slightly positive relationship with increasing CWD until 41 mm and a strong negative relationship with increasing CWD above 41 mm (Fig. 5), as determined through a piecewise regression technique. This response was consistent for both empirical and simulated ANPPs under all four modeling scenarios. ANOVA results demonstrate that this differential response in ANPP above and below this CWD cutoff point is significant ($F = 5.27$, $p = 0.024$).

The LowM-noBB scenario consistently had the highest median ANPP values, whereas the HiM-BB had the lowest median ANPP values (Fig. 5). The regression slopes of the two scenarios that did not include bark beetles had a stronger negative response to higher CWD values (slopes: LowM-noBB = –11.1, HiM-noBB = –9.9) than those scenarios that included bark beetles (slopes: LowM-BB = –7.3, HiM-BB = –6.8), as well as the tree-ring scenario. ANCOVA results reveal that the ANPP~CWD relationships from the model scenarios are statistically different from one another, both below the CWD cutoff ($F = 10.6$, $p \ll 0.005$) and above it ($F = 17.6$, $p \ll 0.005$) (Supplementary material A, Table S8[1]).

Discussion

Forest productivity is influenced by a number of biotic and abiotic factors in conifer forests of the Sierra Nevada, including available soil moisture (Dolanc et al. 2013) and natural disturbances (bark beetle outbreaks, wildfire), as well as land-use legacies (past clear-cutting) and management (forest thinning for fuels reduction). By comparing our simulated ANPP results with empirical ANPP estimates from tree-core data during a time period with multiple interacting disturbances, we were able to quantify how bark beetles and moisture sensitivity influenced the relationship of ANPP to CWD.

CWD thresholds for mortality via cavitation have been demonstrated in certain species in western mixed conifer forests, and predictive models of species mortality built on these thresholds perform well at landscape scales (Anderegg et al. 2015). Similarly, our tree ring derived ANPP estimates indicate a similar inflection point when CWD = ~41, beyond which moisture stress causes a rapid decrease in site-scale growth rate across this landscape (Fig. 5). The relationship between growth rate and moisture stress becomes strongly negative above this value, suggesting that moisture availability becomes the primary limiting factor. Although

Fig. 4. Comparison of empirical aboveground net primary productivity (ANPP) data with four LANDIS-II model scenarios: LowM-noBB, low moisture sensitivity and no bark beetle outbreaks; LowM-BB, low moisture sensitivity and bark beetle outbreaks; HiM-noBB, high moisture sensitivity and no bark beetle outbreaks; and HiM-BB, high moisture sensitivity and bark beetle outbreaks. Each line represents the median ANPP (tree ring, n = 52; LANDIS-II scenarios, n = 31 291), and the shaded areas around each median line represent bootstrapped 95% confidence intervals, 500 draws each. The peach-shaded area is the bootstrapped confidence interval for the "Tree ring" scenario.

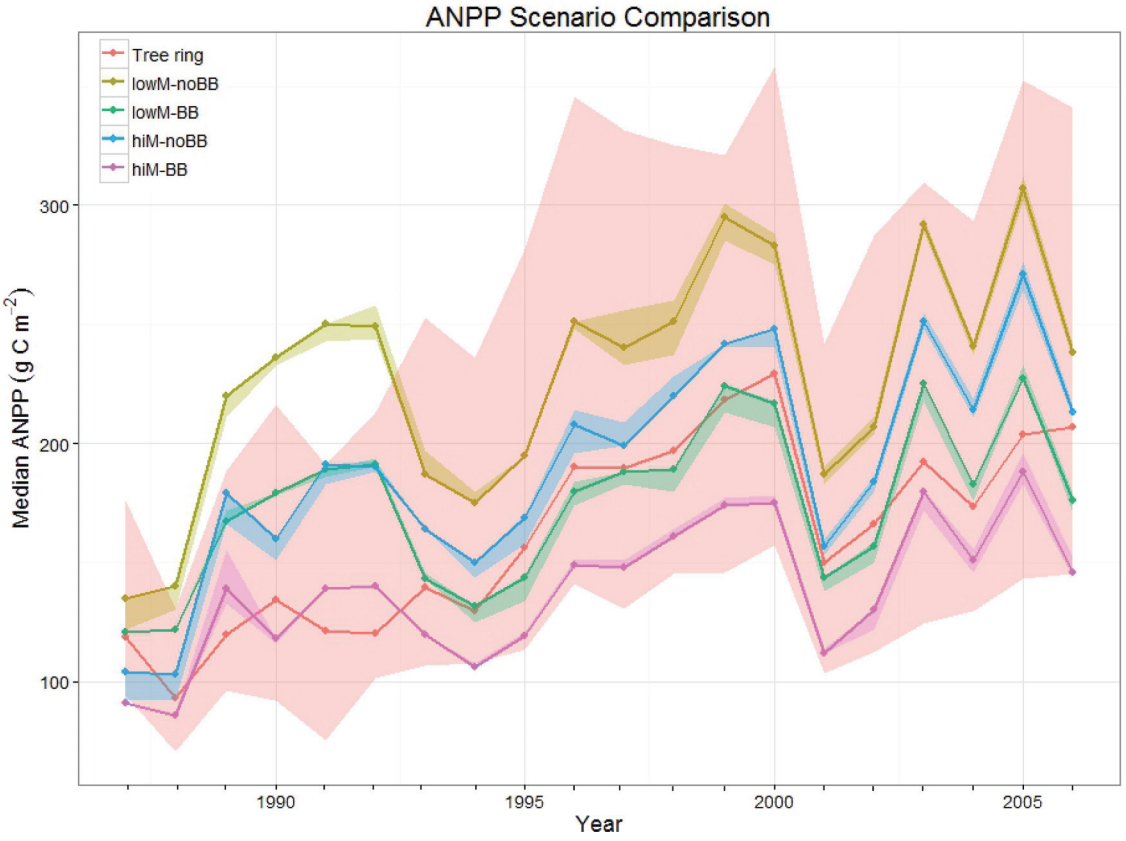

simulated with different drought and beetle parameterizations, the ANPP~CWD relationships calculated from the four LANDIS-II scenarios show a similar change at the same CWD values.

There is a fundamental difference in approach among our model scenarios that include bark beetles (BB) and those that do not include bark beetles (noBB). Physiological responses to climate alone drove ANPP in the absence of bark beetles, whereas climate and beetle-induced mortality drove ANPP in scenarios that included bark beetles. Therefore, a fundamental question about the chosen complexity of the modeling approach must be answered, namely what is gained by including bark beetles and the attendant uncertainty? Landscape models require difficult choices and trade-offs (e.g., complexity vs. parsimony) and with increased complexity comes increased interaction of processes and potential for unintended system outcomes (Gustafson 2013). However, increased complexity is also able to address the emergence of multiscale drivers and incorporate ecological processes that may be more important in the future than they are now. This balance is particularly important if landscape models are to be used to gain meaningful insights into the effects of global climate change (Gustafson 2013).

Year to year, the two scenarios that most closely approximated the field-based ANPP data were the LowM-BB and HiM-noBB scenarios (Fig. 4). However, when looking at growth rate as a function of moisture stress, the LowM-BB scenario had a more similar response to empirical ANPP with increasing CWD than the HiM-noBB scenario (Fig. 5). Furthermore, the regression slopes of the two scenarios that excluded bark beetles (LowM-noBB = –11.1; HiM-noBB = –9.9) were more negative with increasing CWD than the scenarios that included beetles (LowM-BB = –7.3; HiM-BB = –6.1) and the slope for the empirical relationship (–7.5). ANPP differences between the no beetle and beetle scenarios, averaged 53.2 g C·m^{-2} over the course of the 20 year period, which is within the range of productivity reduction observed by MODIS in beetle outbreaks in mixed conifer systems in Colorado (Bright et al. 2013).

Lower parameterized moisture sensitivity, coupled with the simulation of bark beetles (LowM-BB scenario), provides a more mechanistic representation of the coupled processes affecting forest productivity during this timeframe because of the clear biological link of drought and beetle attack (Guarín and Taylor 2005; Hebertson and Jenkins 2008; Creeden et al. 2014) and the prevalence of bark beetles in the LTB (Bradley and Tueller 2001; Walker et al. 2007; Egan et al. 2010). Excluding bark beetles, given their known occurrence, fails to capture the biological feedbacks in the system and ignores a critical disturbance agent that causes forest mortality with subsequent long-term effects on succession and species composition. This is supported by other inventory-based studies, which demonstrate that MPB, in particular, is an episodic control on forest growth and carbon sequestration (Stinson et al. 2011). Although the HiM-noBB scenario may be a more parsimonious model than the LowM-BB scenario, it may be misleading to represent this landscape as a highly moisture-sensitive system not influenced by bark beetle outbreaks rather than the opposite, despite the increased model complexity. Furthermore, where drought-induced bark beetle outbreaks are common, the inclusion of both factors is important for long-term simulations of realistic climate–forest dynamics. For instance, the pulse type disturbance of bark beetle outbreaks and insect–host specificity can create landscape patterns of mortality, recovery, and ANPP different from those from a press type disturbance such as climate-induced moisture stress (e.g., Simard et al. 2012).

Fig. 5. Median aboveground net primary productivity (ANPP) as a function of mean annual climatic water deficit (CWD), as calculated by the Basin Characterization Model. Regression lines show distinction between moisture sensitivity at low moisture stress levels (low CWD) and high moisture stress levels (high CWD). For definitions of scenarios, see caption of Fig. 4.

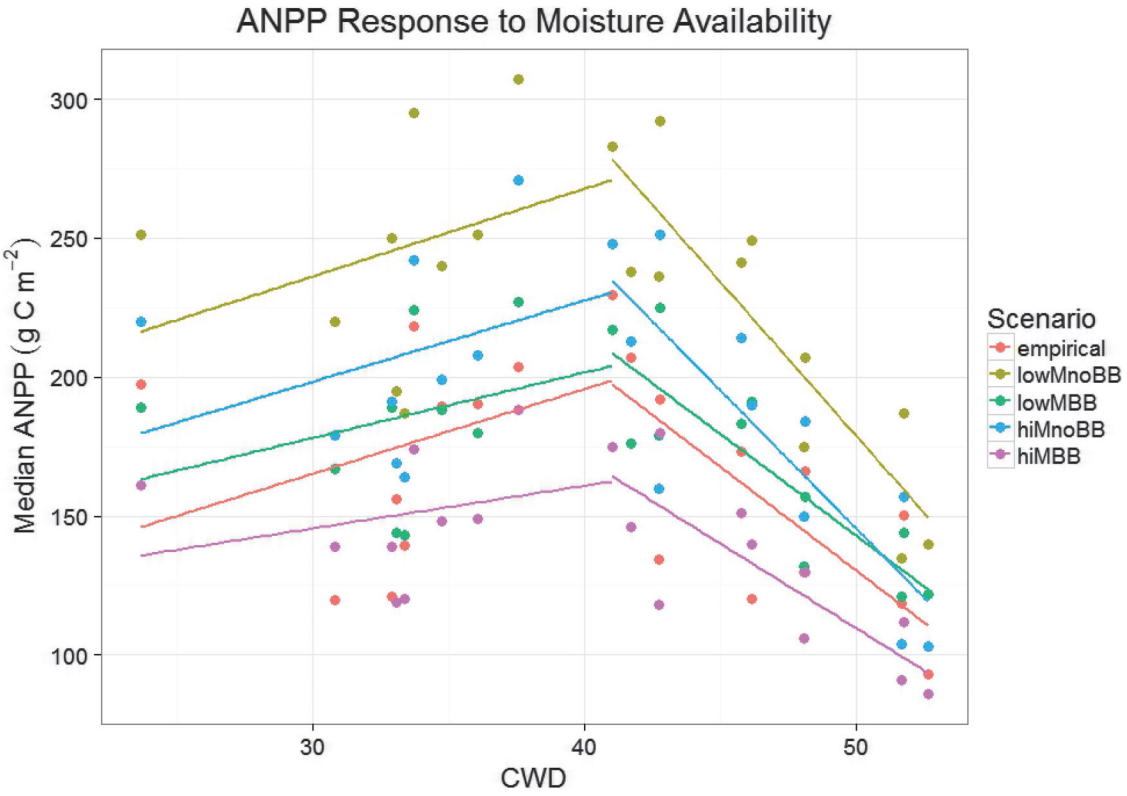

Finally, our use of tree-ring estimates of ANPP provide a novel and critical validation for projections of ANPP, particularly where eddy covariance flux towers (e.g., Scheller et al. 2011) are lacking or inventory sampling is too infrequent to capture important year-to-year variation. Such data assimilation approaches provide the opportunity to improve models and their forecasts by leveraging information on past and current states of an ecosystem (Luo et al. 2011) and are becoming increasingly critical as expectations for model projections of management outcomes increase (Clark et al. 2001).

Our results should be considered in the context of the limitations of both the empirical and simulation approaches. Our empirical ANPP estimates are potentially limited because they do not account for trees that died within plots prior to the sampling period. Live tree mean basal area was 44.2 $m^2 \cdot ha^{-1}$ (standard error = 12.8 $m^2 \cdot ha^{-1}$) and standing dead tree mean basal area was 8.8 $m^2 \cdot ha^{-1}$ (standard error = 7.9 $m^2 \cdot ha^{-1}$). Our empirical ANPP estimates do not include productivity from trees that were alive for only part of the 20 year period, because many of the standing dead trees were not physically sound and able to be extracted. This may account for the 3 years in which the LowM-BB and HiM-noBB scenario estimates were higher than the empirical estimate.

Although we explored two processes that influence ANPP at multiple scales, many critical processes were excluded by design or by necessity in the simulation model. Wildfires and forest thinning were not included in our simulations because there was no evidence of recent fire or thinning practices within the stands selected for tree coring. Although dispersal and host preferences are included, insect physiology is not directly modeled within the BDA extension. Therefore, climate influence on insect population development and dynamics are absent from this study. In our study, we sought to match the temporal and overall spatial patterns of an observed outbreak; therefore, the known drought trigger of beetle outbreaks was incorporated. By deterministically setting the outbreak duration, our simulations do not include beetle climate sensitivities, which could have revealed significant changes to reproductive success during warmer periods, similar to Jonsson et al. (2012). Stochastic behavior was expressed through site selection of beetle mortality, which is influenced by food resources on and around that site. Previous research has shown that mortality rates differ amongst tree size and age classes; effects that are further augmented by stand density (Egan et al. 2016). Our simulations account for these differences by determining different susceptibility rates of species–age classes. However, factors that determine an individual tree's likelihood of being killed (e.g., infestation by red turpentine beetle, placement in a particularly dense stand, microsite enhancement of drought stress) are not explicitly represented within our model, which operates on species–age cohorts. If these factors were taken into consideration, we likely would have seen higher variability of within-stand mortality emerge, as individual trees would have been affected rather than entire cohorts.

Management relevance

Our results are particularly relevant to basin-wide management given the additive effects of disturbance and climate on white fir dominated areas — the primary target species for extensive fuel treatments (Syphard et al. 2011). In many of the stands with the highest potential ANPP, white fir comprises more than 50% of the basal area. This highly productive and prolific seeder is more sensitive to drought conditions compared with other species in the region, although fir reproduction in the region continues to be substantial (Hurteau et al. 2007; Earles et al. 2014). Fir-dominated stands, in general, show a rapid growth potential, and yet, sensitivity to moisture limitation and insects add a layer of complexity to the existing goals of fuels reduction and carbon sequestration. Management decision-making is further complicated by the more

frequent and prolonged periods of moisture stress projected for the region (Coats et al. 2013), notwithstanding the potential for more climate–disturbance feedbacks (Loudermilk et al. 2013).

Conclusions

Our cross-scale comparison demonstrates that representing the effects of both climate and bark beetles on tree growth produces a high level of agreement between simulated and empirical estimates of ANPP. Furthermore, our forest growth analysis suggests that both climatic and disturbance influences should be considered when estimating or projecting ANPP. The limitations on forest growth at the landscape scale are complex, with biotic and abiotic factors playing unique, yet often confounding, roles. Regional climate trends may influence productivity over large areas, but this is often coupled with biotic triggers of insect outbreaks that induce mortality and shift community composition at subregional scales. Deconstructing the relative contributions of each of these factors is important for evaluating model robustness, and using the combination of empirical and simulated data improves projections of future forest dynamics. Ecosystem models can capture the effects of these various influences at scales unavailable to most field studies — a critical capacity for projecting growth patterns into the future changing world.

Acknowledgements

This research was supported using funds provided by the Bureau of Land Management through the sale of public lands as authorized by the Southern Nevada Public Lands Management Act (SNPLMA). The USDA Forest Service, particularly Tiffany van Huysen and Carl Skinner of the Pacific Southwest Research Station, were integral to this work through their support and guidance. We thank Peter Weisberg, University of Nevada-Reno, and Megan Creutzberg, Portland State University, as well as colleagues at the Dynamic Ecosystems and Landscapes Lab at Portland State University. The analysis and writing of this paper was funded in part by the Strategic Environmental Research and Development Program (project RC-2243). We also thank Portland State University for administrative support.

References

Adams, H.D., Guardiola-Claramonte, M., Barron-Gafford, G.A., Villegas, J.C., Breshears, D.D., Zou, C.B., Troch, P.A., and Huxman, T.E. 2009. Temperature sensitivity of drought-induced tree mortality portends increased regional die-off under global-change-type drought. Proc. Natl. Acad. Sci. U.S.A. **106**: 7063–7066. doi:10.1073/pnas.0901438106.

Anderegg, W., Flint, A., Huang, C., Flint, L., Berry, J., David, F., Sperry, J., and Field, C. 2015. Tree mortality predicted from drought-induced vascular damage. Nat. Geosci. **8**: 367–371. doi:10.1038/ngeo2400.

Beaty, R.M., and Taylor, A.H. 2008. Fire history and the structure and dynamics of a mixed conifer forest landscape in the northern Sierra Nevada, Lake Tahoe Basin, California, U.S.A. For. Ecol. Manage. **255**: 707–719. doi:10.1016/j.foreco.2007.09.044.

Bentz, B.J., Régnière, J., Fettig, C.J., Hansen, E.M., Hayes, J.L., Hicke, J.A., Kelsey, R.G., Negrón, J.F., and Seybold, S.J. 2010. Climate change and bark beetles of the Western United States and Canada: direct and indirect effects. BioScience, **60**: 602–613. doi:10.1525/bio.2010.60.8.6.

Bivand, R., Keitt, T., and Rowlingson, B. 2015. rgdal: bindings for the geospatial data abstraction library. R package version 0.9-2. Available from http://CRAN.R-project.org/package=rgdal.

Bontemps, J.D., and Bouriaud, O. 2014. Predictive approaches to forest site productivity: recent trends, challenges and future perspectives. Forestry, **87**: 109–128. doi:10.1093/forestry/cpt034.

Bradley, T., and Tueller, P. 2001. Effects of fire on bark beetle presence on Jeffrey pine in the Lake Tahoe Basin. For. Ecol. Manage. **142**(1–3): 205–214. doi:10.1016/S0378-1127(00)00351-0.

Bright, C.B., Hicke, J.A., and Meddens, A.J.H. 2013. Effects of bark beetle-caused mortality on biogeochemical and biogeophysical MODIS products. J. Geophys. Res. **118**(3): 974–982. doi:10.1002/jgrg.20078.

Bunn, A., Korpela, M., Biondi, F., Campelo, F., Merian, P., Qeadan, F., and Zang, C. 2015. dplR: dendrochronology program library in R. R package version 1.6.3. Available from http://R-Forge.R-project.org/projects/dplr/.

California Landscape Conservation Cooperative. 2011 California Basin Characterization Model (BCM) Downscaled Climate and Hydrolo 30-year Summaries. Available from http://climate.calcommons.org/dataset/10 [accessed November 2015].

Campbell, J., Alberti, G., Martin, J., and Law, B.E. 2009. Carbon dynamics of a ponderosa pine plantation following a thinning treatment in the northern Sierra Nevada. For. Ecol. Manage. **257**: 453–463. doi:10.1016/j.foreco.2008.09.021.

Cantarello, E., Newton, A.C., Hill, R.A., Tejedor-Garavito, N., Williams-Linera, G., López-Barrera, F., Manson, R.H., and Golicher, DJ 2011. Simulating the potential for ecological restoration of dryland forests in Mexico under different disturbance regimes. Ecol. Model. **222**: 1112–1128. doi:10.1016/j.ecolmodel.2010.12.019.

Chen, P.Y., Welsh, C., and Hamann, A. 2010. Geographic variation in growth response of Douglas-fir to interannual climate variability and projected climate change. Glob. Chang. Biol. **16**: 3374–3385. doi:10.1111/j.1365-2486.2010.02166.x.

Clark, J.S., Carpenter, S.R., Barber, M., Collins, S., Dobson, A., Foley, J.A., and Pringle, C. 2001. Ecological forecasts: an emerging imperative. Science, **293**(5530): 657–660. doi:10.1126/science.293.5530.657.

Coats, R., Costa-Cabral, M., Riverson, J., Reuter, J., Sahoo, G., Schladow, G., and Wolfe, B. 2013. Projected 21st century trends in hydroclimatology of the Tahoe Basin. Clim. Change, **116**: 51–69. doi:10.1007/s10584-012-0425-5.

Cole, W.E., and Amman, G.D. 1980. Mountain pine beetle dynamics in lodgepole pine forests. Part 1: course of an infestation. USDA Forest Service, Intermountain Forest and Range Experiment Station, General Technical Report INT-89.

Creeden, E.P., Hicke, J.A., and Buotte, P.C. 2014. Climate, weather, and recent mountain pine beetle outbreaks in the western United States. For. Ecol. Manage. **312**: 239–251. doi:10.1016/j.foreco.2013.09.051.

Daly, C., Taylor, G., and Gibson, W. 1997. The prism approach to mapping precipitation and temperature. Oregon State University, Corvallis, Oregon.

Dolanc, C.R., Thorne, J.H., and Safford, H.D. 2013. Widespread shifts in the demographic structure of subalpine forests in the Sierra Nevada, California, 1934 to 2007. Glob. Ecol. Biogeogr. **22**: 264–276. doi:10.1111/j.1466-8238.2011.00748.x.

Earles, J.M., North, M.P., and Hurteau, M.D. 2014. Wildfire and drought dynamics destabilize carbon stores of fire-suppressed forests. Ecol. Appl. **24**: 732–740. doi:10.1890/13-1860.1.

Egan, J.M., Jacobi, W.R., Negron, J.F., Smith, S.L., and Cluck, D.R. 2010. Forest ecology and management forest thinning and subsequent bark beetle-caused mortality in northeastern California. For. Ecol. Manage. **260**: 1832–1842. doi:10.1016/j.foreco.2010.08.030.

Egan, J.M., Sloughter, J.M., Cardoso, T., Trainor, P., Wu, K., Safford, H., and Fournier, D. 2016. Multi-temporal ecological analysis of Jeffrey pine beetle outbreak dynamics within the Lake Tahoe Basin. Population Ecology. In press. doi:10.1007/s10144-016-0545-2..

Ferrell, G.T. 1994. Predicting susceptibility of white fir during a drought-associated outbreak of the fir engraver, *Scolytus ventralis*, in California. Can. J. For. Res. **24**(2): 302–305. doi:10.1139/x94-043.

Fisichelli, N.A., Frelich, L.E., and Reich, P.B. 2012. Climate and interrelated tree regeneration drivers in mixed temperate–boreal forests. Landsc. Ecol. **28**: 149–159. doi:10.1007/s10980-012-9827-z.

Flint, L., and Flint, A. 2012. Downscaling future climate scenarios to fine scales for hydrologic and ecological modeling and analysis. Ecol. Process. **1**(1): 2. doi:10.1186/2192-1709-1-2.

Flint, L., Flint, A., Thorne, J., and Boynton, R. 2013. Fine-scale hydrologic modeling for regional landscape applications: the California Basin Characterization Model development and performance. Ecol. Process. **2**(1): 25. doi:10.1186/2192-1709-2-25.

Fritts, H.C., and Swetnam, T.W. 1989. Dendroecology: a tool for evaluating variations in past and present forest environments. Adv. Ecol. Res. **19**: 111–188. doi:10.1016/S0065-2504(08)60158-0.

Graf, M. 1999. Plants of the Tahoe Basin. Sacramento, California Native Plant Society Press, California.

Guarín, A., and Taylor, A.H. 2005. Drought triggered tree mortality in mixed conifer forests in Yosemite National Park, California, USA. For. Ecol. Manage. **218**: 229–244. doi:10.1016/j.foreco.2005.07.014.

Gustafson, E.J. 2013. When relationships estimated in the past cannot be used to predict the future: using mechanistic models to predict landscape ecological dynamics in a changing world. Landsc. Ecol. **28**: 1429–1437. doi:10.1007/s10980-013-9927-4.

Gustafson, E.J., and Sturtevant, B.R. 2012. Modeling forest mortality caused by drought stress: implications for climate change. Ecosystems, **16**: 60–74. doi:10.1007/s10021-012-9596-1.

Hebertson, E.G., and Jenkins, M.J. 2008. Climate factors Associated with historic spruce beetle (Coleoptera: Curculionidae) outbreaks in Utah and Colorado. Environ. Entomol. **37**: 281–292. doi:10.1093/ee/37.2.281.

Hijmans, R.J. 2015. raster: geographic data analysis and modeling. R package version 2.3-33. Available from http://CRAN.R-project.org/package=raster.

Holmes, R.L. 1983. Computer-assisted quality control in tree-ring dating and measurement. Tree-Ring Bull. **43**: 69–78.

Hurteau, M., Zald, H., and North, M. 2007. Species-specific response to climate reconstruction in upper-elevation mixed-conifer forests of the western Sierra Nevada, California. Can. J. For. Res. **37**(9): 1681–1691. doi:10.1139/X07-028.

Hurteau, M.D., Robards, T.A., Stevens, D., Saah, D., North, M., and Koch, G.W. 2014. Modeling climate and fuel reduction impacts on mixed-conifer forest carbon stocks in the Sierra Nevada, California. For. Ecol. Manage. **315**: 30–42. doi:10.1016/j.foreco.2013.12.012.

Jenkins, J.C., Chojnacky, D.C., Heath, L.S., and Birdsey, R.A. 2004. Comprehensive Database of Diameter-based Biomass Regressions for North American Tree Species. USDA Forest Service, Northeastern Research Station, General Technical Report NE-319.

Jonsson, A.M., Schroeder, L.M., Lagergren, F., Anderbrant, O., and Smith, B. 2012. Guess the impact of *Ips typographus*—an ecosystem modelling approach for simulating spruce bark beetle outbreaks. Agric. For. Meteorol. **166–167**: 188–200. doi:10.1016/j.agrformet.2012.07.012.

Klutsch, J.G., Negrón, J.F., Costello, S.L., Rhoades, C.C., West, D.R., Popp, J., and Caissie, R. 2009. Stand characteristics and downed woody debris accumulations associated with a mountain pine beetle (*Dendroctonus ponderosae* Hopkins) outbreak in Colorado. For. Ecol. Manage. **258**: 641–649. doi:10.1016/j.foreco.2009.04.034.

Kuijper, D.P.J., Cromsigt, J.P.G.M., Jedrzejewska, B., Miscicki, S., Churski, M., Jedrzejewski, W., and Kweczlich, I. 2010. Bottom-up versus top-down control of tree regeneration in the Bialowieza Primeval Forest, Poland. J. Ecol. **98**: 888–889. doi:10.1111/j.1365-2745.2010.01656.x.

Kurz, W., Dymond, C.C., Stinson, G., Rampley, G.J., Neilson, E.T., Carroll, A.L, Ebata, T., and Safranyik, L. 2008. Mountain pine beetle and forest carbon feedback to climate change. Nature, **452**: 987–990. doi:10.1038/nature06777.

Law, B.E., Turner, D., Campbell, J., Sun, O.J., Van Tuyl, S., Ritts, W.D., and Cohen, W.B. 2004. Disturbance and climate effects on carbon stocks and fluxes across western Oregon USA. Glob. Chang. Biol. **10**: 1429–1444. doi:10.1111/j.1365-2486.2004.00822.x.

Loudermilk, E.L., Scheller, R.M., Weisberg, P.J., Yang, J., Dilts, T.E., Karam, S.L., and Skinner, C. 2013. Carbon dynamics in the future forest: the importance of long-term successional legacy and climate-fire interactions. Glob. Chang. Biol. **19**: 3502–3515. doi:10.1111/gcb.12310.

Loudermilk, E.L., Stanton, A., Scheller, R.M., Dilts, T.E., Weisberg, P.J., Skinner, C., and Yang, J. 2014. Effectiveness of fuel treatments for mitigating wildfire risk and sequestering forest carbon: a case study in the Lake Tahoe Basin. For. Ecol. Manage. **323**: 114–125. doi:10.1016/j.foreco.2014.03.011.

Luo, Y., Ogle, K., Tucker, C., Fei, S., Gao, C., LaDeau, S., Clark, J.S., and Schimel, D.S. 2011. Ecological forecasting and data assimilation in a data-rich era. Ecol. Appl. **21**: 1429–1442. doi:10.1890/09-1275.1.

Mladenoff, D.J., Host, G.E., Boeder, J., and Crow, T.R. 1996. LANDIS: a spatial model of forest landscape disturbance, succession, and management. *In* GIS and environmental modeling. *Edited by* M.F. Goodchild, L.T. Steyart, B.O. Parks, C. Johnston, D. Maidment, M. Crane, and S. Glendinning. GIS World Books Publisher. pp. 175–180.

Muggeo, V.M. 2003. Estimating regression models with unknown break points. Stat. Med. **22**(19): 3055–3071. doi:10.1002/sim.1545.

Pan, Y., Birdsey, R.A., Fang, J., Houghton, R., Kauppi, P.E., Kurz, W., Phillips, O.L., Shvidenko, A., Lewis, S.L., Canadell, J.G., Ciais, P., Jackson, R.B., Pacala, S.W., McGuire, A.D., Piao, S., Rautiainen, A., Sitch, S., and Hayes, D. 2011*a*. A large and persistent carbon sink in the world's forests. Science, **333**: 988–993. doi:10.1126/science.1201609.

Pan, Y., Chen, J.M., Birdsey, R., McCullough, K., He, L., and Deng, F. 2011*b*. Age structure and disturbance legacy of North American forests. Biogeosciences, **8**: 715–732. doi:10.5194/bg-8-715-2011.

Parton, W.J., Anderson, D.W., and Cole, C.V. 1983. Simulation of soil organic matter formation and mineralization in semiarid agroecosystems. The University of Georgia, College of Agriculture Experiment Stations, Athens, Georgia. pp. 533–550.

R Core Team. 2015. R: a language and environment for statistical computing. R Foundation for Statistical Computing, Vienna, Austria. Available from http://www.R-project.org/.

Rogers, J.H. 1974. Soil survey Tahoe Basin Area: California and Nevada. Washington, DC.

Scheller, R.M., Domingo, J.B., Sturtevant, B.R., Williams, J.S., Rudy, A., Gustafson, E.J., and Mladenoff, D.J. 2007. Design, development, and application of LANDIS-II, a spatial landscape simulation model with flexible temporal and spatial resolution. Ecol. Model. **201**: 409–419. doi:10.1016/j.ecolmodel.2006.10.009.

Scheller, R.M., Van Tuyl, S., Clark, K.L., Hom, J., and La Puma, I. 2011. Carbon sequestration in the New Jersey pine barrens under different scenarios of fire management. Ecosystems, **14**: 987–1004. doi:10.1007/s10021-011-9462-6.

Simard, M., Powell, E.N., Raffa, K.F., and Turner, M.G. 2012. What explains landscape patterns of tree mortality caused by bark beetle outbreaks in Greater Yellowstone? Glob. Ecol. Biogeogr. **21**: 556–567. doi:10.1111/j.1466-8238.2011.00710.x.

Skovsgaard, J.P., and Vanclay, J.K. 2008. Forest site productivity: a review of the evolution of dendrometric concepts for even-aged stands. Forestry, **81**: 13–31. doi:10.1093/forestry/cpm041.

Stinson, G., Kurz, W.A., Smyth, C.E., Neilson, E.T., Dymond, C.C., Metsaranta, J.M., Boisvenue, C., Rampley, G.J., Li, Q., White, T.M., and Blain, D. 2011. An inventory-based analysis of Canada's managed forest carbon dynamics, 1990–2008. Glob. Chang. Biol. **17**: 2227–2244. doi:10.1111/j.1365-2486.2010.02369.x.

Stokes, M.A., and Smiley, T.L. 1968. An introduction to tree ring dating. The University of Chicago Press, Chicago, Illinois.

Sturtevant, B.R., Gustafson, E.J., Li, W., and He, H.S. 2004. Modeling biological disturbances in LANDIS: a module description and demonstration using spruce budworm. Ecol. Model. **180**: 153–174. doi:10.1016/j.ecolmodel.2004.01.021.

Suarez, M.L., and Kitzberger, T. 2010. Differential effects of climate variability on forest dynamics along a precipitation gradient in northern Patagonia. J. Ecol. **98**: 1023–1034. doi:10.1111/j.1365-2745.2010.01698.x.

Swanson, M.E. 2009. Modeling the effects of alternative management strategies on forest carbon in the *Nothofagus* forests of Tierra del Fuego, Chile. For. Ecol. Manage. **257**(8): 1740–1750. doi:10.1016/j.foreco.2009.01.045.

Syphard, A.D., Scheller, R.M., Ward, B.C., Spencer, W.D., and Strittholt, J.R. 2011. Simulating landscape-scale effects of fuels treatments in the Sierra Nevada, California, USA. Int. J. Wildl. Fire, **20**: 364–383. doi:10.1071/WF09125.

Temperli, C., Bugmann, H., and Elkin, C. 2013. Cross-scale interactions among bark beetles, climate change, and wind disturbance: a landscape modeling approach. Ecol. Monogr. **83**(3): 383–402. doi:10.1890/12-1503.1.

Thompson, J.R., Foster, D.R., Scheller, R., and Kittredge, D. 2011. The influence of land use and climate change on forest biomass and composition in Massachusetts, USA. Ecol. Appl. **21**: 2425–2444. doi:10.1890/10-2383.1.

Trouet, V., and Taylor, A.H. 2009. Multi-century variability in the Pacific North American circulation pattern reconstructed from tree rings. Climate Dynamics, **35**: 953–963. doi:10.1007/s00382-009-0605-9.

Walker, R.F., Fecko, R.M., Frederick, W.B., Johnson, D.W., and Miller, W.W. 2007. Forest health impacts of bark beetles, dwarf mistletoe, and blister rust in a Lake Tahoe Basin mixed conifer stand. West. N. Am. Nat. **67**: 562–571. doi:10.3398/1527-0904(2007)67[562:FHIOBB]2.0.CO;2.

Wickham, H. 2009. ggplot2: elegant principles for data analysis. Springer New York.